Foam Rheology Near the Jamming Transition

Woldhuis, E.L.

Chapter 2

Bubble Model and Simulations

2.1 Microscopic Model

If a computer model is supposed to represent and describe the transition from an unjammed state to a jammed state, it needs at least two properties. First, the particles in the system need to have some concept of being 'in contact' or not, where forces between contacting particles are stronger than between particles that are not in contact. Second, it needs some 'softness', meaning that particles can still be compressed if they are in contact, so that it makes sense to discuss densities higher than the jamming density.

The simplest of such a system, that has been used extensively in simulations [5,11,27], is a system of discs that exert a hookean (linear) elastic force on each other when they are in contact and that do not interact when not in contact: particles i and j interact via an elastic force $\mathbf{F}^e_{ij}$ given by

$$\mathbf{F}^e_{ij} = k\delta_{ij} \quad d_{ij} < r_{ij} \tag{2.1}$$

$$\mathbf{F}^e_{ij} = 0 \quad d_{ij} > r_{ij}, \tag{2.2}$$

in which k is a spring constant, δ_{ij} is the overlap between bubbles i and j, see figure 2.1, d_{ij} is the distance between (the centers of) bubbles i and j and r_{ij} is the sum of their radii. In addition to satisfying the two minimum demands introduced above (contacts and compressibility), these particles have a number of properties that make them very simple, both conceptually and computationally.

First of all, as shown by Eq. 2.2, these particles only interact when they touch: there is no long range attraction or repulsion. Second, the interactions between the particles are pairwise additive, meaning that the force between particle i and j does not depend on whether particle i is also in contact with

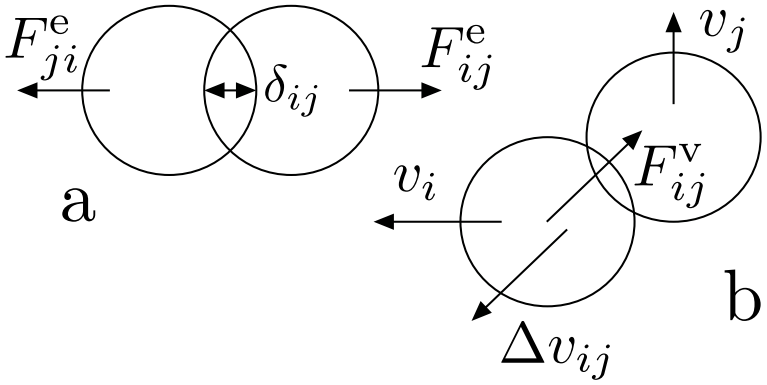

Figure 2.1: **a** two bubbles with a non-zero overlap δ_{ij} exerting forces $F^{\mathrm{e}}_{ij} = k\delta$ on each other. **b** two overlapping bubbles with different velocities v_i and v_j. As a consequence bubble i experiences a velocity difference Δv_{ij} and a force $F^{\mathrm{v}}_{ij} = -b\Delta v_{ij}$. The opposite velocity difference and force working on bubble j are not shown.

other particles. And third, since all forces are central, there are no torques that need to be balanced to attain static equilibrium, only forces. Simulations with these particles are often performed in two dimensions [5, 6, 11] as this allows for a relatively small amount of particles (computationally cheap) with relatively large linear size of the system (to minimise finite size effects) compared to three dimensions. The disadvantage is that monodisperse particles crystallize easily in two dimensions[1]. To counteract this it is customary to use bidisperse discs, with radii with a ratio of 1:1.4, which prevents crystallization [5]. Additionally, previous jamming research suggests that there are no crucial differences between two and three dimensions [5].

The minimum requirements to expand this simple model to flowing or dynamic systems are a means of energy dissipation, to offset the energy put into the system by driving it, and equations of motion, to link forces to velocities. For this, we use Durian's bubble model [27]. In this model, if particles i and j have relative velocity $\Delta\mathbf{v}_{ij}$ they experience a viscous drag $\mathbf{F}^v_{ij}$ given by

$$\mathbf{F}^v_{ij} = -b\Delta\mathbf{v}_{ij} \quad d_{ij} < r_{ij} \tag{2.3}$$
$$\mathbf{F}^v_{ij} = 0 \quad d_{ij} > r_{ij}, \tag{2.4}$$

with b the viscous force constant, see figure 2.1 for a simple illustration. Note that such a force model still only has pairwise additive contact forces, but the viscous force can make discontinuous jumps from zero to a finite value when particles make or break contact, as the viscous force, once in contact, does

[1] because the locally optimal packing, the triangle, can tile space; i.e. there is no frustration [31]

not depend on the overlap. The model takes the equations of motion to be overdamped: forces balance at all time. Since the viscous forces depend on the velocities, this allows the velocities to be determined once the positions are given. Note that, even though the viscous force is not central, we still disregard, as is customary [11, 27], torque balance.

As the name implies, Durian's bubble model was developed to describe collections of bubbles, i.e. foams, though it is also thought to describe emulsions well, since emulsions and foam share many of their important properties [6]. This is also the way we think about our minimal jamming model. Although real foams deviate from the model as described above in several ways, we will argue that these deviations are small in the regimes near jamming that we study. First of all, the amount and arrangement of contacts on a bubble influences the contact force that that bubble will exert on other bubbles due to deformation of the bubble. This effect does not become relevant until very high densities, though, which is why we choose to neglect it. Second, gas bubbles have non-zero mass and therefore will not strictly obey overdamped dynamics. Still, since the mass of gas bubbles is small, bubbles accelerate rapidly and any force imbalance will be very short lived. Finally, bubbles will show some reaction to unbalanced torques, which this model does not take into account. However, bubbles will certainly not rotate as rigid bodies under the effect of torques - at best there will be fluid flow in the interface. In addition it has been shown that the presence or absence of torque balance makes no difference in linear response [32]. Therefore it is reasonable to not include torque balance.

2.1.1 Intermezzo: Roads not Traveled

Besides the microscopic model presented above, we have considered a number of other options that were in the end discarded for various reasons. They are briefly discussed here.

Mean Field Dissipation The method of dissipation described above is not the simplest imaginable. A simpler method was introduced as an approximation by Durian in his original model [27] and has since been used often [11]. This simpler method of dissipation is called 'Mean Field dissipation' and has dissipation take place not when contacting bubbles move relative to each other, as in Eq. 2.3, but when bubbles move relative to the time averaged flow field:

$$\mathbf{F}_i^v = -b\left(\mathbf{v}_i - \mathbf{v}\left(x_i, y_i\right)\right), \tag{2.5}$$

where $\mathbf{v}\left(x_i, y_i\right)$ is the value of the time averaged flow field at the position of particle i. While this approximation was introduced mainly for its computational benefits, it has a clear physical interpretation: viscous drag with the background fluid. Still, in actual foam systems dissipation takes place mostly between bubbles and not between bubbles and the fluid [16].

Therefore we must ask ourselves what the effect of this approximation might be. Since we expect that non-affine flow, which is exactly the flow that gets energetically punished by the mean field dissipation model, is prevalent around jamming, we expect that this approximation will have a large effect. We have nevertheless performed some simulations with the mean field model for comparison and have found that the differences between the two dissipative models are often small. For example, there seem to be few differences between the stresses. For some quantities, however, the differences between the Mean Field and the full Durian model are very big, see for example the correlation lengths in section 2.3.3 and [33].

Overlap-Dependent Viscous Force We know from experiments that the viscous force between bubbles depends not only on their relative velocity, but also on their overlap [34]: if particles have a bigger overlap, they will experience more viscous friction. Therefore, inclusion of this effect into our model would make it more realistic, and could also take away the conceptual problem that results from the fact that the viscous force is discontinuous when contacts are made or broken.

Tangential Friction We have investigated a model in which the viscous force was restricted to the direction perpendicular to the contact/parallel to the contact line: bubbles moving strictly towards or away from each other do not feel any viscous forces, only elastic forces.

This microscopic model has consistency problems, especially since we are doing simulations without inertia. Consider the following situation: bubble A and B are overlapping with each other, but not with any other bubbles. A and B will feel, equal and opposite, elastic forces, acting parallel to the vector connecting their centers. Whatever their relative velocities however, the viscous force that they feel will always be perpendicular to the vector connecting their centers; therefore force balance is impossible, independent of their velocities. Because of these problems, that will not occur often but are hard to overcome when they do, we have implemented a full vectorial dissipative force.

2.2 Simulations

Before we discuss our simulations in depth, it is useful to switch to dimensionless units. There are a number of free parameters in our model, shown in table 2.1, that can be used to construct non-dimensional units for length, time and stress; these can then be used to construct units for any other quantity, such as force or strain rate. As unit of length we pick the radius of the smallest bubbles, r_s, as the bubble size seems more relevant than the system size. We fix the other length scales by using the customary 1:1.4 ratio between small and large bubbles discussed above and by taking a square box with $L_x = L_y = 75$

Parameter		SI unit
width of the system	L_x	m
height of the system	L_y	m
small bubble radius	r_s	m
large bubble radius	r_l	m
spring constant	k	N/m
viscous force constant	b	Ns/m

Table 2.1: Free parameters in our system that set dimensions. k and b are defined in the microscopic force laws of Eqs. 2.1 and 2.3.

which leads, depending on density, to a particle number around 1000. We use k as unit of stress since, in two dimensions, the unit of stress is also N/m. Finally we construct a unit of time as b/k. This is the timescale over which a relative displacement and an overlap of 1 (r_s) result in equal forces. While this is a huge overlap, due to the linearity of the forces this is also the timescale over which a relative displacement and an overlap of 0.1 result in equal forces, etc.

In our simulations we impose a fixed packing fraction, ϕ, and a fixed strain rate, $\dot{\gamma}$, and we measure the stresses that are needed to maintain this driving. We change the packing fraction by changing the number of particles in our system. Since the number of particles has to be an integer, this limits the resolution of our packing fraction to $\frac{\pi 1^2}{75^2} \approx 0.0006$. In order to go beyond this resolution we also slightly change the size of our box to fine-tune the packing fraction and achieve a higher resolution.

We apply a constant strain rate using Lees-Edwards boundary conditions. This means that we use normal periodic boundary conditions in the vertical direction, the direction of flow. But along the horizontal direction, periodic copies of the system are given an extra velocity $\dot{\gamma}L_x$, both for updating the positions of bubbles and for calculating the viscous force over the periodic boundary, see figure 2.2.

2.2.1 Nuts and Bolts

We use a 'forward Euler' iteration scheme for our simulations, which works as follows: at time t we know the positions, $r(t)$, and the velocities, $v(t)$, of all bubbles. To move to the next time step, $t + \delta t$, we then move all bubbles forward with their velocity: $r(t + \Delta t) = r(t) + v(t)\Delta t$. This leads to a new contact network in which we can calculate all elastic forces, as these depend only on position[2]. We can then use the condition of force balance

[2] and the radii, but these are constant and known.

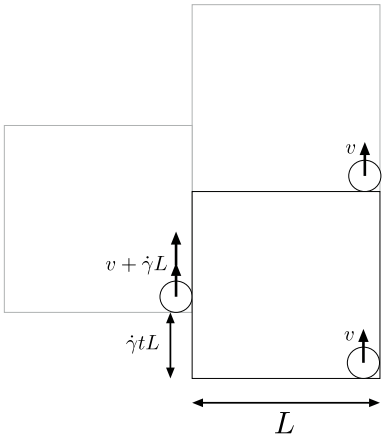

Figure 2.2: Lees-Edwards boundary conditions: particles are simply copied along the vertical, stream wise, direction and are copied with an extra velocity $\dot{\gamma}L$ in the transverse direction.

together with the elastic forces on all bubbles to calculate the velocities of all bubbles, as there is one 2-dimensional unknown velocity and one 2-dimensional force balance constraint per bubble. We use a Newton-Raphson solver for this problem. We now have the positions and velocities of all bubbles at time $t+\Delta t$ and we can repeat the procedure.

We make this mathematically explicit to show why this is computationally more involved than the Mean Field approximation. Let us define the contact matrix $\hat{C}$, this is a Z by N matrix, Z being the total number of contacts between bubbles and N the total number of bubbles in the system. If bubble j is one of the two bubbles in contact i then $\hat{C}_{ij} = 1$ if j has the higher index of the two participating bubbles and -1 if it has the lower[3]. With this definition $\hat{C}\mathbf{V}$, $\mathbf{V}$ being a vector with the velocities of all N bubbles, gives a vector with the relative velocities of all Z contacts. Conversely, applying $\hat{C}^T$ to any vector of contact quantities returns a vector of the sums over all contacts per bubble, i.e. if $\mathbf{F}^e$ is the Z-dimensional vector of elastic forces in each contact, then $\hat{C}^T\mathbf{F}^e$ is the N-dimensional vector of total elastic forces on each bubble. This means that once we have the positions, and therefore the contacts and elastic forces, at time t we need to solve the following equation of force balance for $\mathbf{V}$:

$$\hat{C}^T\left(\mathbf{F}^e - b\hat{C}\mathbf{V}\right) = \mathbf{0} \tag{2.6}$$

This inverse problem is computationally expensive to solve.

In contrast, in the Mean Field approximation the viscous force that a bubble experiences depends only on its own position and velocity, not those

[3]this is an arbitrary sign convention, corresponding with the definition of bond vectors pointing from the lower to the higher index.

of its neighbours. This makes it possible to solve the velocity of each bubble explicitly. If a bubble has a two dimensional velocity[4] $\mathbf{v}$, then the viscous force on that bubble is $-b\left(\mathbf{v}-\dot{\gamma}\hat{\mathbf{x}}r_y\right)$, where $\hat{\mathbf{x}}$ is the unit vector in the x- or flow direction and r_y is the y- or transverse component of the bubble position. If the elastic force on a bubble is $\mathbf{f}^e$, force balance then requires that

$$\mathbf{f}^e - b\left(\mathbf{v}-\dot{\gamma}\hat{\mathbf{x}}r_y\right) = \mathbf{0} \tag{2.7}$$

or $\mathbf{v} = b\mathbf{f}^e + \dot{\gamma}\hat{\mathbf{x}}r_y$, which can be calculated directly since $\mathbf{f}^e$ and r_y are known.

2.3 Phenomenology

In this section we will describe the main phenomenology of the bubble flows from our simulations. Unless otherwise specified we use simulations of approximately 20 units of strain for all strain rates to ensure proper averaging; the transient is typically less then 1.5 units of strain and is excluded from the averaging. Data samples are taken every 2/3 of a percent of strain, for a total of 3000 data points in the full 20 units of strain. The set of densities and strain rates used differs, and will be discussed individually for each result presented below.

2.3.1 Elastic and Viscous stress

Because we use overdamped equations of motion and the forces therefore balance at all times, we can calculate the shear stress needed to get a bubble system flowing from all the forces between the bubbles with the Born-Huang formulation [35]:

$$\sigma_{xy} = \frac{1}{2V}\sum_{<ij>} r_{ij,x} f_{ij,y}, \tag{2.8}$$

here V is the volume of the simulation box, the sum is over all contacting bubbles and r is the contact vector between two bubbles. A similar expression can be formulated for the three other components of the stress, σ_{xx}, σ_{yy} and σ_{yx}. There are two types of forces between the bubbles: elastic forces, as from Eq. 2.1, and viscous forces, as from Eq. 2.3. This means that we can decompose the (shear) stress into two components: the elastic shear stress, σ^{e}_{xy}, due to the elastic forces and the viscous shear stress, σ^{v}_{xy}, due to the viscous forces. Of course, since $f^{\mathrm{e}}_{ij} + f^{\mathrm{v}}_{ij} = f_{ij}$, the elastic and viscous shear stresses taken together give the same stress as calculated in Eq 2.8, which we will call the total (shear) stress, $\sigma^{\mathrm{tot}}_{xy}$. Note also that, since there is no torque balance, $\sigma_{xy} \neq \sigma_{yx}$

Figure 2.3 shows the elastic, viscous and total shear stresses a function of both strain rate (**a**) and density (**b**). As can be seen, the viscous stress

[4] we will now use lower case letters to distinguish two-dimensional vectors from N- or Z-dimensional vectors for which we have used capital letters.

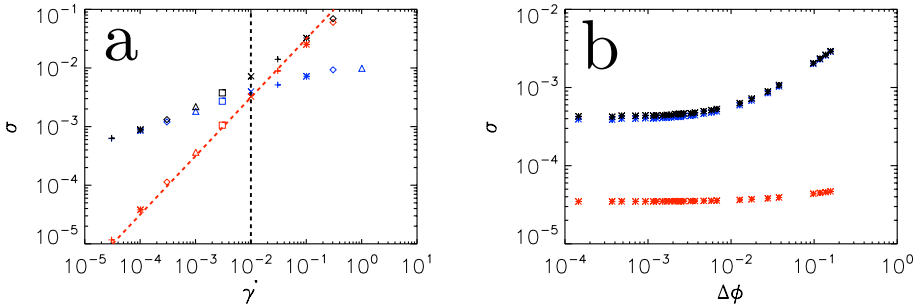

Figure 2.3: The viscous contribution to the stress (red), the elastic contribution to the stress (blue) and the total stress (black). **a**: stresses as function of the strain rate at fixed density ($\phi = 0.87$). The red dotted line indicates linear dependence on strain rate; the black dotted line is our cutoff strain rate. **b**: stresses as a function of density (we have taken $\phi_j = 0.8423$, see section 3.3.2) at a fixed strain rate ($\dot{\gamma} = 10^{-4}$).

is largely independent of the density and scales linearly with the strain rate; it shows newtonian behavior. The elastic stress depends on both the density and the strain rate and, as we will make abundantly clear below, does so in a complicated fashion. Since we can also see from figure 2.3 that the elastic stress tends to dominate the viscous stress, it is clear that any anomalous behavior of the total stress must be caused by the elastic stress. Therefore, in everything that follows we will study the elastic stress only, unless specified otherwise. In order to minimise the effect of the viscous stress, we limit ourselves to those strain rates where the elastic stress dominates the viscous stress: $\dot{\gamma} < 10^{-2}$, left of the dotted black line in figure 2.3. This means that to good approximation, $\sigma^{\mathrm{e}} = \sigma^{\mathrm{tot}}$

2.3.2 Rheological Curves

Above, we have seen that the elastic stress has a complicated dependence on both the strain rate and the density. To get a general feel for this dependence, we plot full strain rate sweeps for three different densities in figure 2.4. We have picked a density that is markedly above the jamming density, $\phi = 0.87$, one that is around the jamming density, $\phi = 0.8424$, and one that is below the jamming density, $\phi = 0.8$.

In the rheological curves of figure 2.4 we recognise a number of different aspects of the rheology of complex fluids that we discussed above. The first aspect is that for the density below jamming, there is newtonian behavior in the limit of small strain rates, indicated by the blue dotted line. The asymptotic behavior at $\phi = 0.87$ is very different though, showing a flattening of the curve,

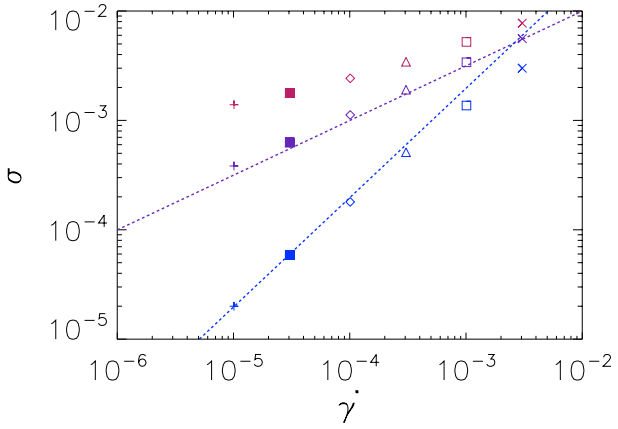

Figure 2.4: The shear stress as a function of strain rate for three different densities: 0.8 (blue), 0.8424 (purple) and 0.87 (pink). All curves approach a similar power law for high strain rate, indicated by the purple dotted line, which has a slope of 1/2. For low strain rates the low density shows steeper behavior and the high density shows flatter behavior. The blue dotted line indicates linear newtonian behavior.

possibly approaching a yield stress plateau[5].

The high strain rate asymptote is also interesting, as here all three densities approach the same behavior, shown by the purple dotted line. In all three cases we see shear-thinning behavior, i.e. a power law with exponent less than one. Moreover this exponent appears to the same for all three densities. At the jamming density this behavior extends all the way to low strain rates; for the densities away from jamming it crosses over into the low strain rate asymptotes discussed before.

All of this is consistent with observations from several other experiments and simulations [11, 24, 27–29]. In fact, Olsson and Teitel have already shown that by rescaling with appropriate powers of $\Delta\phi$ all data can be collapsed onto two branches, one below and one above jamming [11]. In the next chapter we will introduce a scaling model that will predict these exponents, as well as the shear-thinning exponent and a number of other surprising details, from three simple assumptions. We will also find that this way of rescaling the data does not capture the full behavior.

2.3.3 Correlation Length

Another phenomenon that Olsson and Teitel observe is a length scale in the correlation of the non-affine motion. I.e. they calculate the following correla-

[5] though that plateau is not reached

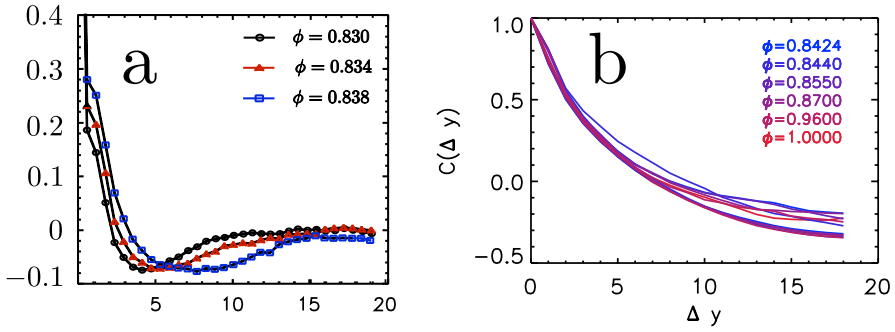

Figure 2.5: Two plots of the non-affine motion correlation length as a function of streamwise displacement. **a**: the original data from Olsson and Teitel [11] from simulations with Mean Field dissipation. **b**: data from our simulations with fully resolved bubble-bubble dissipation; a strain rate of 10^{-5} and $3 \cdot 10^{-3}$ are shown for each density.

tion function:

$$C\left(y\right) = \left\langle v_x(0) v_x(y) \right\rangle , \tag{2.9}$$

where <> denotes averaging over time and over all bubble pairs that are displaced only in the stream wise direction[6], v_x is the x-component, and therefore crosswise component, of the velocity of each bubble. Since there is no movement in the x-direction in the average flow profile, all movement in this direction is non-affine. A length scale, ξ, can be extracted from this correlation length and Olsson and Teitel find that $\xi^{-1} \sim |\Delta\phi|^{0.6} f\left(\sigma/\Delta\phi^{1.2}\right)$, [11]. An example of the correlation functions that they find is shown in figure 2.5 **a**.

When we calculate the same correlation function however, we do not find a length scale that changes with the density, see figure 2.5 **b**. In fact, if we perform simulations for different system sizes, we find that we can collapse the correlation data by simply rescaling with the linear size of the system. Additionally, the shape of our correlation functions looks different from those of Olsson and Teitel [33].

The most striking difference between our simulations and those of Olsson and Teitel is the form of the dissipation. Olsson and Teitel use mean-field dissipation, discussed in section 2.1.1, while we use the bubble-bubble dissipation of the full Durian model. Since this is the biggest difference between the two systems, it is the most likely explanation for the difference. In fact,

[6]The simulation box is divided into several stream wise 'lanes' and bubble velocities are correlated only between bubbles in the same lane, therefore their cross wise displacement is not necessarily zero, but will be bounded from above by the lane width

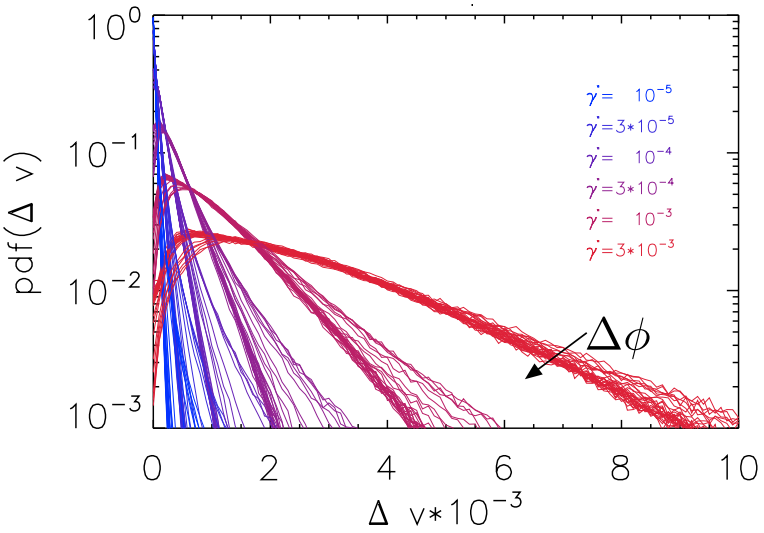

Figure 2.6: The probability distribution function of the relative velocity between particles for different strain rates (color) and different densities ranging from $\phi = 0.8424$ to $\phi = 1$.

if we perform our own simulations with mean field dissipation we recover the Olsson and Teitel correlation functions with their characteristic dip. We cannot fully explain why these two similar systems give such different correlation lengths, especially since most of their other behavior is very similar. However, in a tentative explanation we point to the fact non-affine motion is the source of dissipation in the Mean Field model, but not in the full Durian model. In section 6.1 we show that energy dissipation, which is caused by relative motion between the bubbles[7], sets the (second moment of the) distribution of relative velocities. Therefore it is not unlikely that the non-affine velocity is largely set by considerations of energy dissipation in the Mean Field model, but not in the full Durian model.

We note, however, that the mean field model was introduced as an approximation to the full Durian model under the assumption that it was a harmless computational simplification [27]. As we have shown that there is at least one significant difference between the two models we feel that it is highly preferable to use the full Durian model.

2.3.4 Δv-distributions

The role played by the non-affine velocity in the mean field model, that of source of energy dissipation, is played by the relative velocity in the full Durian

[7] in the full Durian model

model. Due to big differences in the energy supplied to systems of different density or strain rate, there are also big differences in the behavior of the relative velocity. As an example of this we show the probability distribution functions of a wide range of data in figure 2.6. Note the incredible difference in the fatness of the tails of the distributions. These differences lead to wildly different behavior in the systems, an aspect that we will explore in section 6.1.